ELSEVIER

Opthal. Physiol. Opt. Vol. 17, No. 5, pp. 433–440, 1997

0275-5408/97 $17.00 + 0.00

PII: S0275-5408(97)00015-X

TECHNICAL NOTE

Improved computing scheme for measuring eye alignment with Purkinje images I and IV

J. C. Barry,[1] A. Backes,[1] U. M. Pongs,[1] T. Kirschkamp[1] and M. C. M. Dunne[2]

[1]Department of Ophthalmology, Medical Faculty of RWTH Aachen University, Pauwelsstrasse 30, D-52057 Aachen, Germany and [2]Ophthalmic and Physiological Optics Research Group, Vision Sciences, Aston University, Birmingham B4 7ET, UK

Summary

This study introduces an improved computing scheme for determining eye rotation from Purkinje images I and IV. The original computing scheme systematically underestimated eye rotation. Paraxial raytracing calculations revealed that this error resulted from failure to account for the fact that Purkinje images I and IV fall at different distances behind the cornea. The error could be overcome with a correction factor derived from paraxial raytracing calculations. A series of experiments were carried out to test the validity of this correction factor; involving exact raytracing calculations as well as measurements on physical model eyes and human eyes. The influence on the correction factor of ocular surface asphericity, accommodation, age and ocular component variations were examined. The new method was also compared to Hirschberg's technique, which makes use of Purkinje image I alone, as a means of screening for strabismus.

Introduction

Measurement of the relative decentrations of Purkinje images I (reflected from the anterior corneal surface) and IV (reflected from the posterior lens surface) is a useful method of determining rotation of both eyes, especially for the purpose of detecting small angle strabismus (Barry *et al.*, 1992, Barry *et al.*, 1994b). However, this method systematically underestimates the angle of eye rotation by 5% to 10% (Barry *et al.*, 1992, Barry *et al.*, 1994c). This paper examines the causes of the systematic error and introduces an improved computing scheme which preserves the main advantages of the original technique. One of these advantages is that measurements are only required of relative Purkinje image positions in arbitrary units. Calibration is therefore not required. Further, the technique can be applied to digitised images of patients with or without glasses worn, as spectacle magnification will not influence relative measurements. Another of the advantages is that no additional biometric information is required for calculations.

Correspondence to: Dr J. C. Barry at the above address

Received: 29 June 1996
Revised form: 10 February 1997

Methods

The source of the systematic error

The principles of the original computing scheme, described in detail elsewhere (Barry *et al.*, 1992, Barry *et al.*, 1994b), are illustrated in *Figure 1*. This figure depicts Purkinje images I and IV (denoted PI and PIV arising from three horizontally aligned, equidistant light sources each subtending an angle τ_O with respect to the subject's eyes. These light sources are usually

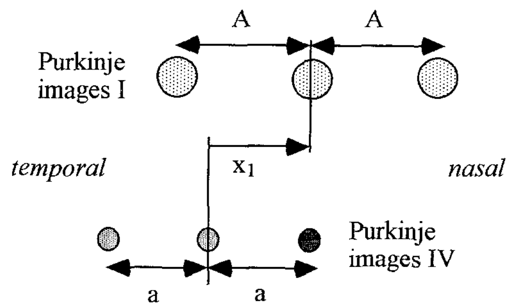

Figure 1. Definition of distances to be measured for the purposes of the computation scheme. The diagram illustrates the typical appearance of Purkinje images I and IV (denoted PI and PIV) arising from the three light sources used by the Purkinje I and IV Reflection Pattern Evaluation technique

positioned eccentrically, above or below the fixation target, to provide good vertical separation of Purkinje images I and IV. Equation (1) describes the calculation of τ_O according to the original computing scheme, where D is the distance between each light source and d is the distance between the central light source and both eyes.

$$\tau_O = \arctan(D/d) \tag{1}$$

Distances x_1, A, and a (shown in *Figure 1*) are measured in arbitrary units which, as previously mentioned, is convenient in the presence of spectacle magnification and removes the need for calibration. The original computing scheme involves determination of angle τ (the angle between each eye's optical axis and the middle light source) using Equation (2):

$$\tau = \tau_O{}^* x_1/(a + A) \tag{2}$$

The angle of strabismus is the difference between the angles τ calculated for the right and left eyes (Barry *et al.*, 1992, Barry *et al.*, 1994b). Therefore, any systematic error present in the calculation of τ pertains equally to the calculated angle of strabismus.

Figure 2 represents a horizontal section through the anterior segment of a schematic eye. This illustrates the positions, determined using paraxial raytracing calculations (Jones and Eskridge, 1970; Brodie, 1987;

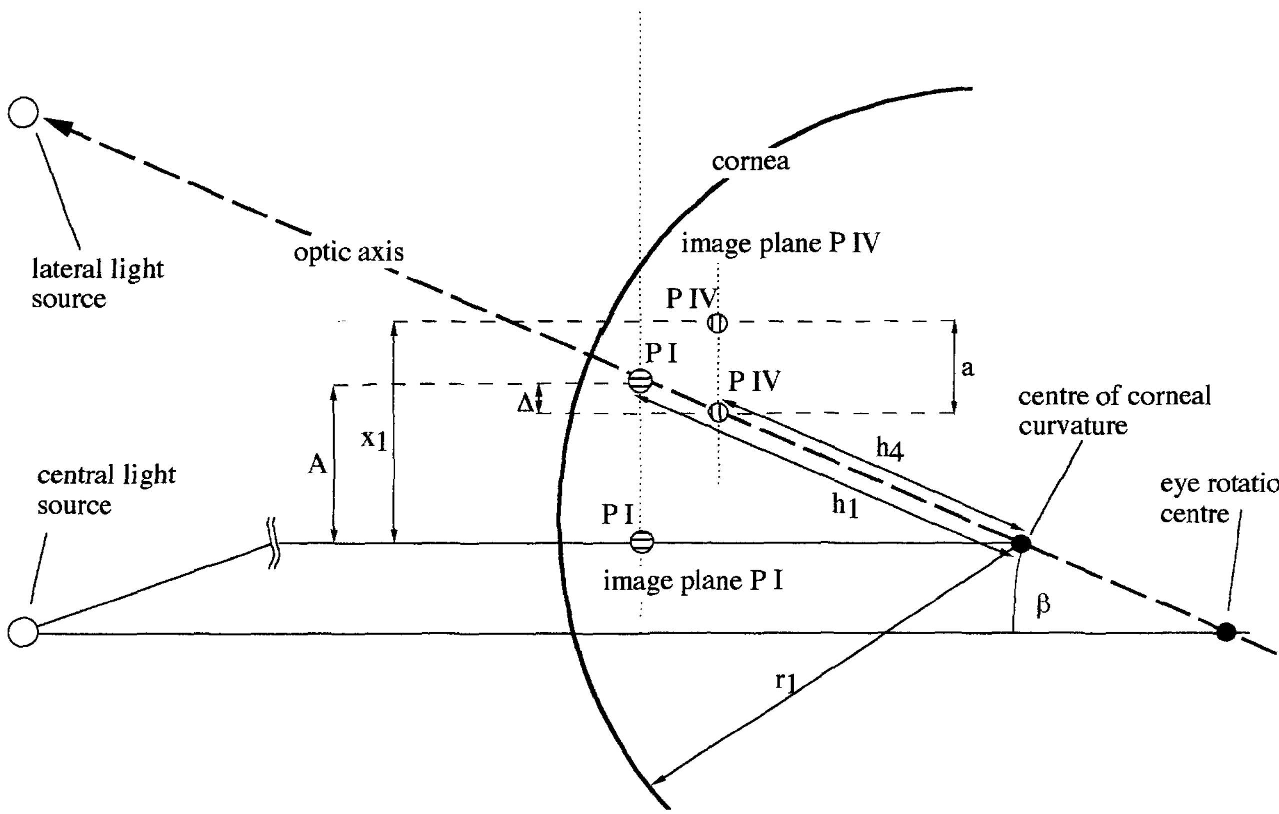

Figure 2. Derivation of the improved computing scheme. This representation of a schematic eye, in horizontal cross section, shows pairs of Purkinje Images I and IV (denoted PI and PIV) calculated using paraxial raytracing calculations. Only two of the three light sources mentioned in *Figure 1* are shown. The eye has been rotated by an angle $\tau_O = \beta$ so that its optical axis is lined up to the lateral light source. This has resulted in Purkinje image displacement

Quick and Boothe, 1992), of Purkinje images I and IV (denoted PI and PIV) arising from the central and a lateral light sources. The eye is rotated by an angle $\beta \approx \tau_O$ such that the optic axis points towards one of the lateral light sources.

The original computing scheme (Equation 2) assumed that $x_1 = A + a$ when $\beta = \tau_O$. However, the distance x_1, as seen by the imaging system placed close to the middle light source, does not exactly equal the distance A + a. Therefore, τ, calculated with Equation (2), does not equal τ_O. In actual fact, Purkinje images I and IV, as seen from the central light source, lie in different axial positions (h_1 and h_4) which, as illustrated in *Figure 2*, causes x_1 to be smaller than A + a by a distance Δ. This explains the systematic underestimation of the true eye rotation angle β found using the original computing scheme.

It is also necessary to calculate the angular subtense τ_O of the light sources as seen through the cornea. In other words, the light source distance required to calculate τ_O should be the true distance d' from the middle light source to the centre of corneal curvature. It is this distance that determines the heights of Purkinje images I and IV. This entails modification of Equation (1) as shown below (Equation 3), where r_1 is the anterior corneal radius.

$$\tau_O = \arctan(D/(d' + r_1)) \tag{3}$$

Derivation of improved computing scheme

The systematic error may now be described in terms of Δ (see *Figure 2*):

$$\Delta = (h_1 - h_4)^*\sin(\beta) \tag{4}$$

To correct Equation (2), Δ is subtracted from a + A which leads to Equation (5):

$$\tau_{corr} = \tau_O{}^*x_1/(a + A - \Delta) \tag{5}$$

In order to obtain a simple expression, a multiplicative correction factor K, is introduced in Equation (2) instead of Δ, which yields Equation (6).

$$\tau_{corr} = K^*\tau_O{}^*x_1/(a + A) \tag{6}$$

Now, from comparison with Equation (5) we derive Equation (7).

$$K = 1/(1 - \Delta/(A + a)) \tag{7}$$

The problem is that Δ is unknown and cannot be measured directly. In the special case depicted in *Figure 2*, $\beta = \tau_O$ which simplifies the numerical evaluation of the correction procedure. Distance Δ is calculated using Equation (4) by substituting τ_O for β. Also, distances $h_1 - h_4$, a and A can be determined by paraxial raytracing through Le Grand's schematic eye (Le Grand and El Hage, 1980). For a light source placed so that $d' = 500$ mm and $\tau_O = 10°$ (a frequently adopted value of τ_O; Barry *et al.*, 1994c) the required values are $h_1 - h_4 = 0.454$ mm, $A = 0.693$ mm, and $a = 0.528$ mm. Using these figures, correction factor $K = 1.0691$, close to the value derived empirically from previous studies (Barry *et al.*, 1992, Barry *et al.*, 1994c). Use of this correction factor may be extended to angles of eye rotation β where the paraxial approximation still holds since the correction factor may be derived in the same manner for any angle $\tau_O \approx \beta$, with identical results.

A useful way of investigating the systematic error arising from the axial separation ($h_1 - h_4$) of Purkinje images I and IV is to consider the angular ratio, s, of measured (τ) versus true (β) eye rotation angles (i.e. $s = \Delta\tau/\Delta\beta$). Logically, if $h_1 - h_4 = 0$ then $s = 1$; if $h_1 - h_4 > 0$ then $s < 1$; if $h_1 - h_4 < 0$ then $s > 1$ (the latter case means that there is a "reversal" of axial positions of Purkinje images so that PIV is closer to the corneal apex than PI). Paraxial raytracing reveals factors that influence s. For instance, increased anterior chamber depth increases $h_1 - h_4$ so that s reduces and correction factor K increases. Flattening the cornea reduces $h_1 - h_4$ thereby increasing s which, in turn, leads to a reduction in K.

Validation of improved computing scheme

The previous section explained how the systematic error could arise due to failure of the original computing scheme to account for the axial separation of Purkinje images I and IV. Further theoretical and experimental support for this is now provided. The calculations that follow are based upon a light source distance of 477 mm and an angle τ_O of 10.059°.

Measurements on a physical model eye

The aim of this part of the study was to compare angular ratios (s) and correction factors (K) derived from three physical and schematic eye model variants designed to exhibit a range of Purkinje image I and IV axial separations.

A physical eye model was constructed, based on the schematic eye of Le Grand (Barry *et al.*, 1994a). Its Purkinje I/IV image size ratio was –0.750 and the axial separation of Purkinje images I and IV was 0.200 mm (Purkinje image I located closer to the corneal vertex). These quantities approximately match those of Le Grand's schematic eye –0.762, 0.454 mm). The corneal anterior vertex to posterior crystalline lens vertex distance was varied from 7.4 mm (close to Le Grand's value of 7.6 mm) through 8.0 mm to 8.8 mm by means of three different purpose built model eye components (due to technical constraints, no shorter values of the vertex to vertex distance than 7.4 mm could be realized but shorter distances will be examined in the following section).

Measurements taken from the three physical model eyes were compared to the results of paraxial and exact raytracing calculations carried out on three corresponding schematic eyes. As a check, close agreement (error smaller than 1.5%) was found between Purkinje I/IV image size ratios derived from physical and schematic eye models.

Each of the physical model eyes was accurately rotated up to $\pm 20°$ by means of a precision goniometer mounted on an optical bench (both supplied by OWIS, Rödersheim, Germany). Measurements of Purkinje images I and IV were used to calculate eye rotation angles (τ) using Equation (2). Angular ratios (s) were then calculated from the gradient of regression lines fitted to plots of τ versus true eye rotation angle β. The reciprocal of each angular ratio then yielded experimental correction factors (K_{exp}).

Similarly, Purkinje images derived from each of the schematic eyes were used to calculate angular ratios from which theoretical correction factors were derived. Calculations involved either paraxial raytracing (yielding K_{parax}) or exact raytracing (yielding K_{exact}). Exact raytracing was carried out using a computing scheme described elsewhere (Barry *et al.*, 1997).

Table 1 compares the correction factors (K_{exp}, K_{parax} and K_{exact}) calculated for the three eye variants. For each eye variant, the anterior corneal vertex to posterior crystalline lens vertex distance is shown along with the resulting Purkinje image I to IV axial separation ($h_I - h_4$). Only small differences (less than 1.5%) were found between correction factors arising from the physical eye and those arising from the schematic eyes applying either paraxial or exact raytracing.

These results indicate that simple paraxial raytracing calculations offer a suitable means of deriving correction factors for the improved computing scheme. The results also demonstrate that changing the anterior corneal vertex to posterior crystalline lens vertex primarily influences the axial separation of Purkinje images ($h_I - h_4$) which, in turn, alters the angular ratio (s) and the required correction factor (K).

Effect of corneal asphericity on the validity of the paraxially derived correction factors

In the previous section, the validity of the paraxially determined correction factor was tested on model eyes with spherical surfaces. However, the human eye comprises aspheric surfaces. For example, a typical value for corneal asphericity is given by an eccentricity factor $Q = -0.15$ (Guillon *et al.*, 1986), which describes a surface that becomes progressively flatter in the periphery. We have previously observed a reduction of the angular ratio (s) for large eye rotation angles. This part of the study therefore investigates whether corneal asphericity might be the cause of this additional systematic error which is not accounted for using the paraxially determined correction factor.

Exact raytracing (Barry *et al.*, in press) was carried out on Le Grand's schematic eye with corneal Q-factors ranging from 0 (spherical surface) through −0.15 to −0.3 and for a light source configuration with $\tau_O = 10°$. The standard distance (7.6 mm) between the anterior corneal vertex and the posterior crystalline vertex of Le Grand's schematic eye was adopted together with two variants with distances of 6.6 mm and 8.6 mm; achieved by varying the anterior chamber depth.

As for the previous section, the computed positions of Purkinje images I and IV were used to calculate eye rotation angles (τ) using Equation (2). Angular ratios (s) were then determined from regression lines fitted to plots of τ versus true eye rotation angle (β) up to $\pm 10°$ (representing small eye rotations) and $\pm 25°$ (representing large eye rotations).

As an aside, raytracing revealed that correction factors (K_{parax} and K_{exact}) still exceeded unity for an anterior corneal vertex to posterior lens vertex distance of 6.6 mm. Technical constraints had prevented us from investigating the effect of this variant of the physical model eye. Further, concordance between paraxial and exact raytracing values was as good as shown for other eye variants in *Table 1*.

Table 1. Comparison of correction factors derived from exact raytracing (K_{exact}), paraxial raytracing (K_{parax}) and from physical model eye (K_{exp}) measurements with three anterior corneal vertex to posterior crystalline lens vertex distances ($V_{AC} - V_{PL}$) and corresponding axial separations ($h_1 - h_4$), rounded to significant figures

$V_{AC} - V_{PL}$/mm	$h_1 - h_4$/mm	K_{parax}	K_{exact}	K_{exp}
7.4	0.20	1.03	1.03	1.02
8.0	0.85	1.14	1.14	1.12
8.8	1.77	1.32	1.34	1.32

The main finding for this part of the study was that, for eye rotations within $\pm 10°$ only small differences ($<0.2\%$) in angular ratio emerged from schematic eye variants with spherical corneae compared to those with aspheric corneae.

Considering eye variants with spherical corneae, angular ratios calculated for small rotation angles (within $\pm 10°$) differed only slightly ($\leq -1\%$) from values calculated for large rotation angles (within $\pm 25°$). As expected for large rotation angles, a slight systematic decrease of the angular ratio ($\leq -1.5\%$) was observed when comparing eye variants with spherical corneae to those with aspheric corneae ($Q = -0.3$). It therefore follows that, for typical human eyes, a higher correction factor (K) would be needed for the investigation of eye rotation angles beyond $\pm 10°$. Nevertheless, when the paraxially derived correction factor ($K = 1.096$) was applied to all eye varients, with and without aspheric corneae, the resulting angular ratios differed by $<-3\%$ from the ideal ratio 1. Therefore, the use of the standard correction factor would lead to a fairly small systematic underestimation of eye rotation.

Effect of accommodation on the correction factor

With accommodation the anterior crystalline lens surface steepens more than the posterior lens surface and the posterior lens vertex remains in nearly the same position (Gilmartin, 1995). Paraxial raytracing revealed that 2 D of accommodation, modelled in the three schematic eye variants, gave rise to a small ($<1\%$) reduction of the correction factor.

Age dependence of the correction factor

Biometric data from the literature (Gordon and Donzis, 1985;Mutti *et al.*, 1995) were used to model a typical one-year-old and six-year-old eye. Components for a two-year-old eye were estimated by interpolation. The six-year-old eye closely resembled that of an adult so that the correction factor was almost exactly the same ($K_{parax} = 1.066$) as for Le Grand's eye ($K_{parax} = 1.069$). Correction factors of $K_{parax} = 1.009$ and $K_{parax} = 1.032$, were calculated for one- and two-year-old eyes, respectively.

This means that K is likely to increase up to about four to five years of age. In children under one year of age, use of the standard correction factor is likely to overestimate eye rotation. To compensate for this, an age-dependent correction factor derived from interpolation of the values stated above could be used in children up to six years of age: $K = 0.993485 + 0.019637*\text{age}$ (in years) or $+0.0012131*\text{age}$ (in months).

However, systematic errors resulting from use of the standard correction factor are fairly small compared to interindividual variations of the correction factor, addressed next.

Interindividual variations of the correction factor

Correction factors were determined for nine variants of Le Grand's schematic eye. These eye variants were designed to represent the full range of ocular component variation found in adult human eyes and are very similar to the variants of Gullstrand's schematic eye previously described by Bennett and Rabbetts (1989).

The axial separation of Purkinje images I and IV ($h_1 - h_4$) varied from -1.18 mm (Purkinje image IV in front of I) to 1.89 mm (Purkinje image IV behind I) in these eye variants. Consequently, the correction factor varied between 0.874 and 1.440. Normalized to the standard correction factor ($K = 1.069$), the percentage variation ranged from -19% to $+32\%$. The resulting range of angular ratios ($s = 1/K$) exceeded our previously determined empirical range (Barry *et al.*, 1992, Barry *et al.*, 1994c) which fell within $\pm 20\%$ (95% confidence interval determined from measurements on 62 subjects). This indicated that the eye variants provided a good estimate of the biometric variations likely to be encountered and, therefore, it was reasonable to assume that variation of the correction factor should not exceed 20–25%. This is an estimate of the maximum inherent error due to biometric component variation when the standard correction factor is applied to all eyes. We assume that the same degree of inherent error also applies to very young eyes.

Measurements in human eyes

Range of measurable eye rotations

We wished to determine the measurable range of eye rotations using our technique (involving measurement of Purkinje images I and IV) compared to the well known Hirschberg technique (involving measurement of only Purkinje image I).

Three measurements were taken from nine right eyes. The light sources were set up so that angle $\tau_O = 10°$. Corrected eye rotation angles calculated using Purkinje images I and IV, are shown in *Figure 3*a for the entire range of eye rotations possible, in the subject with the largest asphericity ($Q = -0.28$) found in the study.

Applying Hirschberg's technique involved estimating eye rotation angles from the measured distance between the central corneal reflex (see *Figure 1*) and the pupil centre. Measured distances were converted to

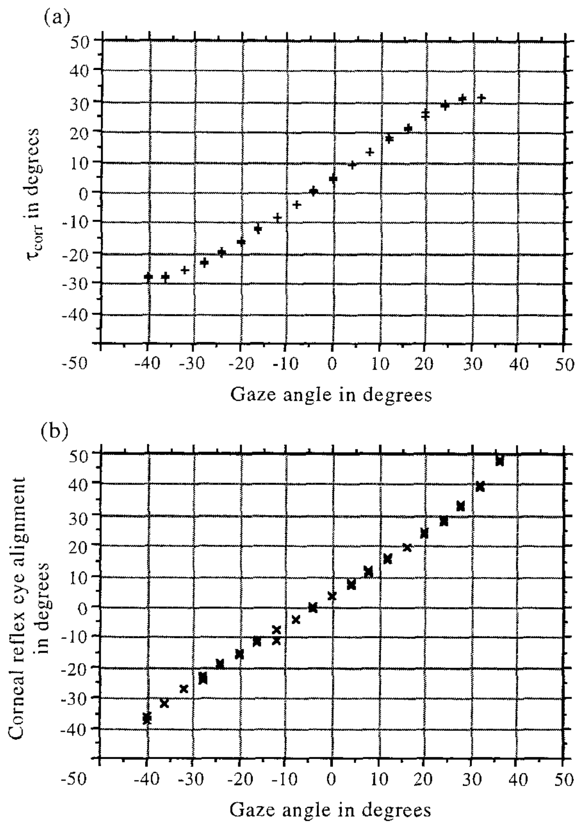

Figure 3. Eye rotation angles measured using (a) Purkinje images I and IV or (b) Purkinje image I alone in a right eye for the full range of nasal (negative) and temporal (positive) gaze angles in one of the nine subjects

estimated eye rotation angles adopting a Hirschberg ratio of 21 PD/mm (11.85°/mm), which was determined from regression lines fitted to measured corneal reflex displacements versus eye rotations up to ±20°. *Figure 3*b shows eye rotation angles estimated using this technique in the same subject.

The graph of calculated (τ_{corr}) versus true (β) eye rotation (*Figure 3*a) is linear for angles within ±20°. The angular ratio (s) obtained by calculating the slope of the regression line fitted to this portion of the data ($s = \Delta\tau/\Delta\beta$) is close to the paraxial angular ratio ($S_{parax} = 1/K_{parax}$). For gaze angles larger than ±20°, however, the angular ratio decreases. This further confirms that underestimation of eye rotation angles beyond ±20° must be expected when a standard, paraxial, correction factor is used.

Beyond eye rotations of 30° nasally and 25° temporally, no reliable measurement of eye rotation was feasible with a light source subtense of $\tau_O = 10°$. At these limits, one of the lateral light sources would be imaged by the corneal periphery on the corneoscleral limbus and would thus become distorted. The asymmetry of these limits results from angle kappa.

Use of the central corneal reflex to determine eye rotation (Hirschberg technique) allowed measurements to be taken from a further 10° nasally and temporally. As mentioned earlier, calculated eye rotations were based upon a Hirschberg ratio determined for eye rotations within ±20°. Therefore, a fairly linear relationship between calculated and actual eye rotations was found within this range (*Figure 3*b). For larger eye rotations, however, the slope of the curve increased. This indicates that an overestimation of large eye rotations must be expected if a constant Hirschberg ratio is adopted.

For both techniques, the non-linearities are likely to have arisen from corneal asphericity and inadequacies of paraxial assumptions involved in the calculation of eye rotation. Considering the latter of these, for example, the change in slope (*Figure 3*a) for larger eye rotations could not be predicted using the paraxially determined correction factor.

Clearly, a narrower range of measurable eye rotations is possible using Purkinje images I and IV compared to use of Purkinje image I alone (Hirschberg's technique). As a rule of thumb, the difference is equal to angle τ_O.

Improvement of estimated eye rotation achieved using new computing scheme

We wished to assess the level of improvement achievable with the new computing scheme. Ten orthotropic subjects (most were moderately myopic) were measured for gaze angles up to ±18.8° at 50 cm fixation distance and with light sources set up so that $\tau_O = 10°$. Angular ratios (s) were calculated as previously described. As no significant differences were found between mean ratios determined in right and left eyes (unpaired *t*-test carried out to 95% significance level), the mean uncorrected angular ratios for right and left eyes were pooled. Before correction, a mean angular ratio of 0.924 emerged with 95% of the sample failing within ±0.099 of this value. After correction with the standard factor K = 1.069, the mean angular ratio was closer to unity (0.987, with 95% of the sample falling within ±0.103 of this value). It follows that empirically determined correction factors are likely to vary by ±10%.

As the subjects in this sample were slightly myopic, their globes are likely to have been larger than average with flatter than average corneal radii (indeed, the mean corneal radius was 8.05 mm which is flatter than the value of 7.8 mm quoted for the typical human eye). As a result of this, the average uncorrected angular ratio in this sample was smaller than for Le

Grand's eye (exact raytracing: 0.944, paraxial raytracing: 0.935). This could explain why the mean corrected angular ratio in this sample was somewhat smaller than the ideal value 1.

Finally, Hirschberg ratios were calculated in this sample in the same manner described in the previous section. The mean ratio was 22.35 PD/mm 12.6°/mm with 95% of the sample falling within ±8.1 PD/mm (±4.6°/mm) of this value. This represents a ±36.5% variation about the mean Hirschberg ratio which is more than three times larger than the variation (±10%) found for the correction factor (K).

Conclusions

The axial separation of Purkinje images I and IV ($h_1 - h_4$) is a major source of the observed systematic underestimation of eye rotation. Exact raytracing and measurements taken from a physical model eye demonstrate that this systematic error can be remedied with a correction factor derived from simple paraxial raytracing calculations. Further, a standard correction factor of K = 1.069 may be applied to adult eyes. Measurements on human eyes and investigations carried out on physical and schematic eye model variants revealed that ocular component variations had a reasonably limited effect on the correction factor.

A further minor source of systematic error should be mentioned here. This results from the fact that the angular subtense of the light sources (the angle formed by lines drawn between the central and lateral light sources and corneal centre of curvature, see *Figure 2*) exceeds the eye rotation angle (the angle formed by lines drawn between the central and lateral light sources and the centre of eye rotation, see *Figure 2*). This difference is not accounted for when applying paraxial calculations and could lead to errors of up to 1% error in angular ratio. This effect could explain some of the differences between the results of paraxial raytracing and those gained from exact raytracing or the physical model eye.

A possible source of systematic error should be addressed for completeness of this study: 1—cyclopean calculation of measured angles of ocular alignment, as used in this study and for calculation of eye alignment, should induce a nasal-temporal asymmetry in our data, since real eyes are decentered which means that eyes rotated inward are really rotated less than the corresponding cyclopean eye, and vice versa for an eye rotated temporally. However, this effect is compensated for by another one occurring with the angles separating the three light sources: 2—the contralateral angle τ_0 as 'seen' by the eye appears smaller, while the ipsilateral one appears larger than the cyclopean angle τ_0, and the change of the distance, x_1, shows the same nasal-temporal asymmetry. Since the distances, A and a, are calculated as average of the contra- and ipsilateral distances (see *Figure 1*), they equal the cyclopean angle τ_0 closely. Consequently, the net effect of 1 combined with 2 is negligible.

Comparison with corneal reflex techniques

The link between the axial separation of Purkinje images I and IV and systematic errors of eye rotation has an analogy in corneal reflex methods, such as Hirschberg's technique. For the latter, the corneal reflex and the landmark (i.e. the entrance pupil centre), which serves as a reference point, are also axially separated. The distance (h), between the centre of corneal curvature and the reference point, determines Hirschberg's ratio. This ratio is described as millimeters of corneal reflex displacement (x) per degree of eye rotation (β) by the relationship $x/h = \sin\beta$ (Jones and Eskridge, 1970). Empirical calibration of Hirschberg's ratio may be performed in order to find the best average ratio in a representative sample (Brodie, 1987). Here, Hirschberg's ratio (for corneal reflex techniques) is analogous to the angular ratio (for techniques using Purkinje image I and IV) as both govern eye rotation estimates in similar ways.

While theoretical analysis of corneal reflex techniques reveals that Hirschberg's ratio depends on the ocular dimensions of the anterior segment (Eskridge *et al.*, 1990), there is little experimental evidence for the range of Hirschberg's ratio. A study in infants showed that 95% of the variation of Hirschberg's ratio fell within ±10 PD/mm (5.7°/mm) of the mean (Riddell *et al.*, 1994). This variation is 50% of the typical value for Hirschberg's ratio (21 PD/mm). We have reported a much smaller range for our angular ratio, based on physical and schematic eye model variants and experimental evidence. This indicates that techniques utilizing the corneal reflex alone are more prone to biometric variation than those utilizing Purkinje images I and IV.

Proper use of correction factors

The present study revealed two major findings. Firstly, the standard correction factor was close to unity and, for eye rotations within ±20°, did not vary much with age and accommodation. Secondly, ocular component variations had a greater effect on the correction factor, although still reasonably limited, than either accommodation or age.

One could, from a practical point of view, neglect the systematic differences altogether and not use a correction factor at all. This could be the right way to proceed in the age group two to three years, which, from a screening point of view is the preferred target group when the technique is applied for strabismus screening. In adults, however, the use of the standard correction factor is strongly recommended.

If measurements over a wide range of ages were to be compared, then an age-dependent correction factor could be useful. If one chooses to use an age-dependent correction factor, its value should be checked and updated when new data are available. Presently, data on infants and children and the modelling of an age-dependent equivalent refractive index (Mutti *et al.*, 1995) are still somewhat tentative.

In the case of detection of small angles of strabismus ($\pm 5°$), for which the method was designed, a systematic error of 5% to 7% translates into an absolute error of 0.25° to 0.35°. This may seem negligible. However, when repeated measurements are averaged or used to compute a strabismus index (Barry *et al.*, 1996), as is the case when the method is used for screening, fractions of a degree of systematic error can influence the decision to refer. Consequently, the thresholds derived for classification of data should be based on normative data too. An age dependence need not be included in the correction factor itself, since the thresholds used for misalignment detection may be made age dependent themselves.

Finally, the correction factor should be used consistently within the remit of a study or a series of studies. It should also be clearly stated whether a correction factor was used and which one was used. This is essential for the comparison of results.

In conclusion, this study supports the claim that the Purkinje I and IV reflex technique offers a more accurate measurement of eye misalignments within $\pm 20°$ compared to corneal reflex techniques. This is especially the case when considering eye misalignment detection thresholds. Fortunately, digital imaging of three light sources, as described in this paper, allows one the option to determine eye alignment from the corneal reflex alone or in conjunction with Purkinje image IV. This leaves room to use either evaluation technique, depending on which one promises best results under given circumstances. The corneal reflex could be used whenever the Purkinje I and IV technique may not be used reliably; for alignment angles exceeding $\pm 25°$, for when the fourth Purkinje images does not form due to media opacities or for when superimposition of Purkinje images I and IV occurs.

Acknowledgements

DAAD grant 313 ARC VII 93/2 (Barry) and ARC grant 507 (Dunne). Corporate support: Chiron Adatomed Intraocular Lenses, Munich (Germany); National Instruments, Munich (Germany); Management Intelligenter Technologien, Aachen-Kornelimünster (Germany); Graftek, Mirmande (France); Polymer Technologies, Weinheim (Germany); eltec, Mainz (Germany); pro cornea, Erbeek (The Netherlands).

References

Barry, J. C., Effert, R. and Kaupp, A. (1992). Objective measurement of small angles of strabismus in infants and children with photographic Purkinje Reflection Pattern Evaluation. *Ophthalmology 99*, 320–328.

Barry, J. C., Effert, R., Dunne, M. C. M., Baumgarten, J., Wählisch, G., Starke, D. and Reim, M. (1994a). A model eye for testing the accuracy of the measurement of the angle of strabismus with Purkinje Reflection Pattern Evaluation. *Invest. Ophthalmol. Vis. Sci. 35*, S2202.

Barry, J. C., Effert, R., Kaupp, A. and Burhoff, A. (1994b). Measurement of ocular alignment with photographic Purkinje I and IV Reflection Pattern Evaluation. *Invest. Ophthalmol. Vis. Sci. 35*, 4219–4235.

Barry, J. C., Effert, R., Reim, M. and Meyer-Ebrecht, D. (1994c). Computational principles in Purkinje I and IV Reflection Pattern Evaluation for the assessment of ocular alignment. *Invest. Ophthalmol. Vis. Sci. 35*, 4205–4218.

Barry, J. C., Hartmann, A. and Effert, R. (1996). Statistical validation of a strabismus index calculated from objective ocular alignment data. *Strabismus 4*, 57–68.

Barry, J. C., Branmann, K. and Dunne, M. C. M. (1997). Study of catoptric properties of eyes with misaligned surfaces by exact raytracing. *Invest. Ophthal. Vis. Sci. (in press)*.

Bennett, A. G. and Rabbetts, R. B. (1989) *Clinical Visual Optics*. 2nd edn, Butterworths, London, pp. 266-268.

Brodie, S. E. (1987). Photographic calibration of the Hirschberg test. *Invest. Ophthalmol. Vis. Sci. 28*, 736–742.

Eskridge, J. B., Perrigin, D. and Leach, N. E. (1990). The Hirschberg test: correlation with corneal radius and axial length. *Optom. Vis. Sci. 67*, 243–247.

Gilmartin, B. (1995). The aetiology of presbyopia: a summary of the role of lenticular and extralenticular structures. *Ophthal. Physiol. Opt. 15*, 431–437.

Gordon, R. A. and Donzis, P. B. (1985). Refractive development of the human eye. *Arch. Ophthalmol. 103*, 785–789.

Guillon, M., Lyndon, D. and Wilson, C. (1986). Corneal topography: a clinical model. *Ophthal. Physiol. Opt. 6*, 47–56.

Jones, R. and Eskridge, J. B. (1970). The Hirschberg test – a re-evaluation. *Am. J. Optom. 2*, 105–114.

Le Grand, Y. and El Hage, S. G. (1980). *Physiological Optics*. Springer, Berlin, pp. 71-74.

Mutti, D. O., Zadnik, K. and Adams, J. A. (1995). The equivalent refractive index of the crystalline lens in childhood. *Vision Res. 35*, 1565–1573.

Quick, M. W. and Boothe, R. G. (1992). A photographic technique for measuring horizontal and vertical eye alignment throughout the field of gaze. *Invest. Ophthalmol. Vis. Sci. 33*, 234–246.

Riddell, P. M., Hainline, L. and Abramov, I. (1994). Calibration of the Hirschberg Test in human infants. *Invest. Ophthalmol. Vis. Sci. 35*, 538–543.